Analysis of the March 13, 2005 Earthquake in Southeastern Iran Based on Teleseismic and Regional Distances

Mehrdad Mostafazadeh

Seismology Research Centre, International Institute of Earthquake Engineering and Seismology (IIEES), I.R. Iran, email: mehrdad@iiees.ac.ir

ABSTRACT: *The treatment of the seismic source inverse problem, when waveform data are available, is simple and elegant using synthetic seismogram formalism. This study constrains source parameters of the March 13, 2005 earthquake by analyzing body wave seismograms in teleseismic and regional distances. The results from waveform modeling indicate that source depth was 32km and that it was a normal mechanism with a small strike slip component. The duration of source time function (STF) is approximately 5sec. Regional determination of body wave (S) spectra are used to estimate the parameters of seismic moment (M_o=10.45×10^{25}dyne-cm), corner frequency (fo=0.54hz), source dimension (R=2.5km) and stress drop (D_σ = 0.26×10^4 bar). Comparison between obtained results and the Harvard CMT solution data show that there is some difference in common parameters, especially in the depth value and seismic moment (the depth value and seismic moment reported by Harvard is 56km and 1.17× 10^{25}dyne-cm respectively). Scatter in the seismic moment values is caused by such factors as the site conditions and errors in the radiation pattern corrections.*

Keywords: Waveform modeling; Spectra; Saravan

1. Introduction

Much of the mechanical deformation resulting from the Arabia-Eurasia collision is accommodated in the Iran plateau. Specifically, the Saravan Fault system in eastern Iran, see Figure (1), is an active fault of the Sistan-Baluchestan Suture Zone that may accommodate a large proportion of ca 20*mm/yr* right lateral shear between Iran and Afghanistan [1-2].

A study of historical records shows that few destructive earthquakes have occurred in the 100*km* radius of the March 13, 2005 earthquake epicenter. An 1838 event with magnitude M = 7 and 1815 event with magnitude M = 5.5 occurred along the Nosrat-Abad Fault and Saravan Fault, respectively, see Figure (2). In addition, some historical events, especially in the south of the region could be associated with the Makran Subduction Zone (latitude and longitude data is unavailable). Evidently, events in 1483, 1765, and 1851 took place along the western, eastern and central portions of the zone [11].

Records show that a number of large earthquakes with magnitudes greater than 6 have occurred in the Sistan-Baluchestan Suture Zone over the past 30 years. The January 10, 1979 earthquake (M_w = 6.0, centroid time 01:26:9.4 *GMT* and *Mw* = 6.1 centroid time 15:05:50.2) occurred in the Makran Range near the Kishi Fault, see Figure (2). The 1980 earthquake with magnitude M_w = 5.4 occurred in January 1, in the Makran Range near the Maskutan Fault and an earthquake (M_w = 6.6) occurred in the East Iranian Range near the Saravan Fault system on April 18, 1983, see Table (1). The January 14, 2003 earthquake (M_w = 5.4) occurred in the East Iranian Range near Saravan Fault and the June 24, 2003 event (M_w = 5.5) occurred in the Makran Range near the Maskutan Fault, see Figure (2). Moment tensor solutions of these events as reported by Harvard are plotted in Figure (2).

On March 13, 2005, another large earthquake occurred near the Saravan Fault (M_w = 6.0). This study

determined the dynamic characteristics of this earthquake through joint analysis of teleseismic and regional data. Long period *P* and *SH* waveform stations of the Global Digital Seismograph Network (*GDSN*) were used for the far-field analysis. Regional data were taken from digital recording stations of the Iran National Broadband Seismic Network (*INSN*).

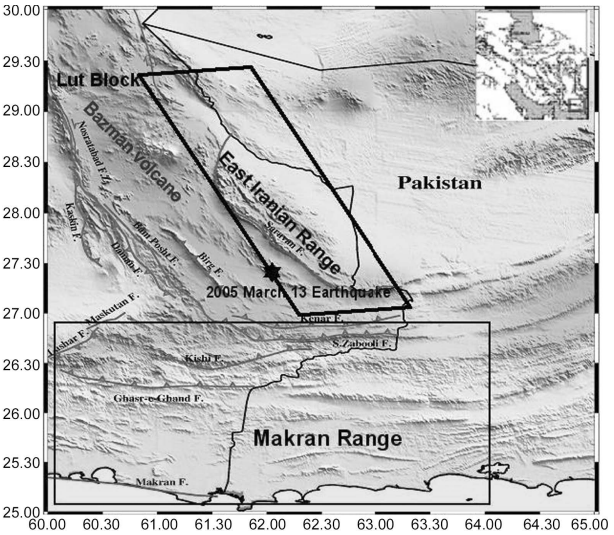

Figure 1. Fault map and location of March 13, 2005 earthquake.

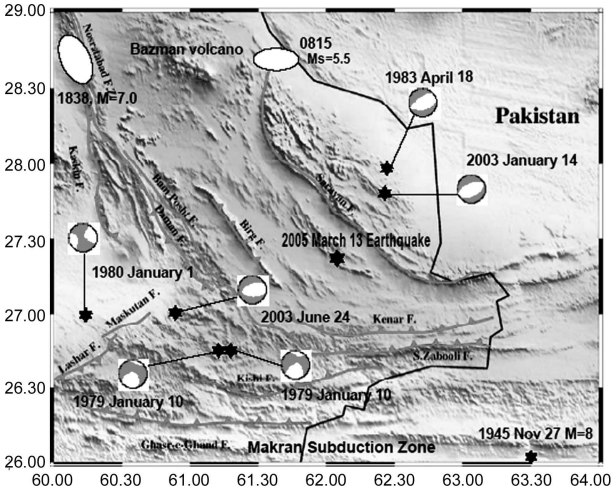

Figure 2. Fault map, some historic earthquakes ( ), and Harvard moment tensor solution of previous earthquakes in the region.

Table 1. Previously recorded earthquakes in Sistan Baluchestan province.

Date (year/month/day)	Origin Time (GMT)	Latitude (N)	Longitude (E).	M_W
1979/01/10	01:26:9.4	26.75	61.23	6.0
1979/01/10	15:05:50	26.75	61.31	6.1
1980/01/01	02:45:57.9	26.99	60.27	5.4
1983/04/18	10:59:2.9	27.94	62.44	6.7
2003/01/14	14:14:2.9	27.77	62.42	5.4
2003/06/24	06:52:55.8	27.00	60.91	5.5
2005/03/13	03:31:27.2	26.82	62.05	6.0

Several investigators have studied earthquake sources by using far-field and near-field data. For example, Choy et al [3-4] used both types of data for the study of earthquake sources in the Northwest Territories, Canada. There are two commonly encountered descriptions of point sources. The first is in terms of an angular description of the nodal planes in the *P* radiation from a purely slip motion on a fault. The second, is the description of the source by the six independent components of the moment tensor, which are assumed to have common dependence on time [5].

The slip on the fault that generates the earthquake is determined by the direction of relative plate motion. The normal to the auxiliary plane then determines the direction of the slip vector. The magnitude of the slip can in principle be determined from the seismic moment, M_O of the earthquake, which can be obtained directly from the seismogram [6].

Body waveform modeling has become one of the most important tools available to obtain strike, dip, rake and centroid depth. In addition it provides more information about the fault-rupturing process. Teleseismic waveform modeling of earthquakes over the past 30 years gives seismic moment precision of about 20 percent [7-8]. The seismic moment, M_O, is a measure of the spectral amplitude of regional data [9]. It is related to two fundamental source parameters, average fault displacement, *D*, fault rupture area, *A*, and rigidity module, μ, [10].

2. Active Tectonics

The eastern part of central Iran is usually divided in two parts, the western Lut Block and a strongly folded eastern part that has been named the East Iranian Range. Active faulting in Iran is related to the convergence between the Eurasia and Arabia plates, which occurs at about 40*mm/yr* at 60°*E* longitude and is mostly accommodated by distributed shortening within the political borders of Iran [12]. While much of this shortening is taken up in the main earthquake and mountain belts of the Zagros, Alborz and Kope Dagh ranges [13], some is also accommodated in central Iran, of which Sistan-Baluchestan province is a part. Recent and active deformation in Sistan-Baluchestan is dominated by *NW* striking thrusts and *N-NNE* striking right-lateral strike slip motion, caused by indentation of Iran by the Arabian shield [14]. The Makran and East Iranian Ranges along the Afghanistan-Pakistan border are

post-Cretaceous flysch belts that join in *SE* Iran and continue into the Pakistan Baluchestan Range. The Makran Range exhibits seismicity that is consistent with the interpretation of this region as a zone of active subduction. Apparently the Bazman active volcanic-arc in the Lut Block is associated with this subduction zone, see Figure (1). A great earthquake ($Ms=8$) occurred in this region in 1945 [15].

3. Analysis Procedure

3.1. Waveform Modeling of the March 13, 2005 Earthquake

To provide constraints on the source parameters of the March 13, 2005 Saravan earthquake, the *P* and *SH* waveforms were analyzed. Digital long period records were taken from *GDSN* stations in the epicentral range of 30°-90°. All waveforms were low-passing filtered (Butterworth) at a cut-off frequency of 0.2*Hz* to remove high frequency components that may cause instability during inversion. The *IASPEI SYN*4 algorithm [16], which is a recent version of Nabelek's [17] inversion procedure based on a weighted least squares method, was used for waveform inversion. The results of this inversion are shown in Figure (3) and Table (2). The solution indicates lateral motion on a fault dipping 37° with a strike of 53°.

To estimate uncertainties in source parameters, an inversion was carried out with the strike, dip, and rake fixed to the Harvard values, see Table (3), but with the depth, time function and moment free. The quality of fit between observed and synthetic seismograms was then visually examined to detect deterioration from the minimum misfit solution. In this way, the uncertainty in strike, dip, rake and depth was estimated for each event. This procedure gives a more realistic quantification of likely errors than the formal errors derived from the covariance matrix of the solution (comparison of observed and synthetic data for different depths, as shown in Figure (4)).

An elastic attenuation for the teleseismic synthetics is accounted for by the Futterman *Q* operator [18] with constant $t^* = T/Q$ [19], where T is the ray travel time and *Q* is the average seismic quality factor along the ray. For *P* waves, a t^* of 1 and, for *SH* waves, 4.0 was used [8]. This methodology is illustrated in greater detail by Molnar and Lyon-Caen [20] and Taymaz et al [8]. Uncertainties in t^* lead to uncertainties in source duration and seismic moment, but only have a small effect on centroid depth and source orientation [21].

Bases for the choice of the crustal model in this study are the same model as is used by Maggi et al [21] and Walker et al [22] for the southeastern Iranian plateau. Here, a 35*km* crust of average *P* velocity of 6.8*km/s* and a half space mantle of *P* velocity 8*km/s* was used.

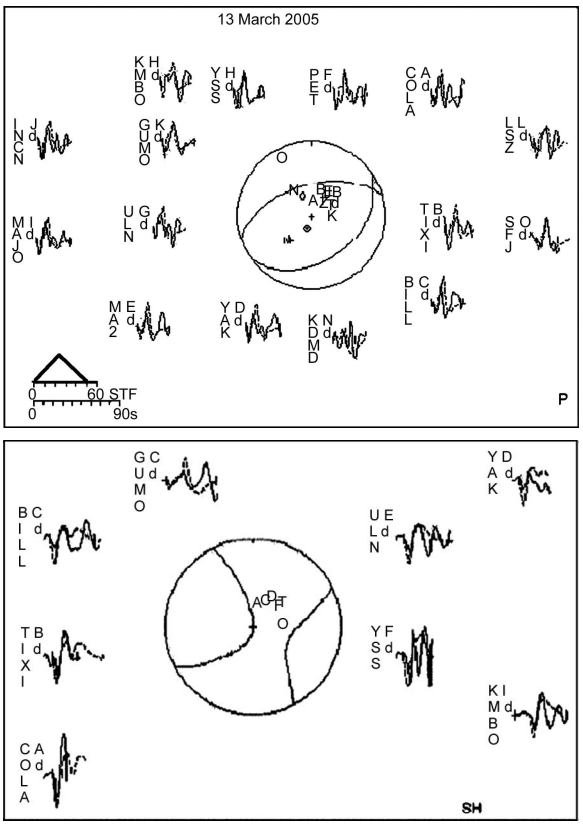

Figure 3. The P and SH radiation patterns of minimum misfit solutions for the main shock of the March 13, 2005 earthquake. Solid lines = observed waveform; dotted lines = synthetic data. The station code is to the left of each waveform. Lower case letters indicate the type of instrument (d = GDSN long period).

Table 2. Source parameters for March 13, 2005 earthquake obtained from waveform modeling.

March 13, 2005	Strike	Dip	Rake	Depth	Source Duration (sec)	Seismic Moment (NM)
Nodal Plane 1	252±11	55±12	282±8	32±5	5	1.23e+18
Nodal Plane 2	53±11	37±12	-	-	-	-

Table 3. Source parameters for March 13, 2005 earthquake reported by Harvard (CMT).

March 13, 2005	Strike	Dip	Rake	Depth
Nodal plane 1	253	37	-89	58
Nodal plane 2	72	53	-90	-

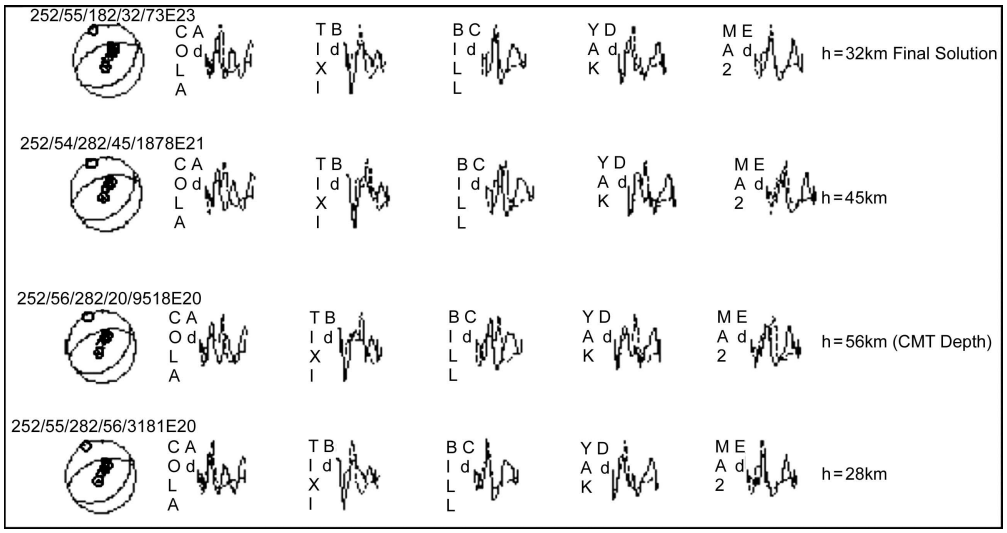

Figure 4. A selection of waveforms from a run of the inversion program and the P focal sphere for the focal parameters (strike, dip, rake, depth, seismic moment). The station code is to the left of each waveform. Solid lines = observed waveform; dotted lines = synthetic data.

3.1.1. Source Time Function (STF)

The teleseismic *STF* gives information about fault ruptures or source complexity. The physical features of teleseismic *STF* appraise the source complexity of earthquakes. These features include the overall duration, multiple or single event character, individual source pulse widths, and roughness of the time function. The *STF* is represented by a set of overlapping isosceles triangles. The base of each tringle has a length of 2τ (τ = the half duration) and a height that is determined by the inversion [17].

The *STF* of this earthquake, with a total duration of 5s, shows simple characteristics, see Figure (3). This shock can be associated with a single rupture. Shallow earthquakes inside the continent show simple *STF*, in general, corresponding to a simple impulse of triangular form with short time duration.

3.2. Regional Data Analysis

In such procedures, values for earthquake moments must first be estimated by spectral analysis or integration of displacement records. In addition, methods based on coda wave analysis have been applied for moderate sized earthquakes [23-24]. The purpose of such methods is to allow the evaluation of the seismic moment using one of them, thereby reducing the need for spectral analysis. It would be preferable, of course, to base the estimation of M_O on records from broadband seismographs [25]. The theoretical foundation for the proposed method comes from the well-known analytical expression derived by Keilis-Borok [26] and has already been applied to a number of earthquakes:

$M_O = 4\pi\mu\rho\beta D W_0 / 2R\theta\phi$, where μ ($3.1\times10^{11} dyne\text{-}cm$) is rigidity, ρ ($2.9 gr/cm^3$) is the density, β ($3.7 km/sec$) is the shear wave velocity, $R\theta\phi$ depends on the source radiation pattern (assumed 1.6, [27], and D is the hypocentral distance from the source. The physical meaning of W_o is the product of pulse width and amplitude and is closely related to the mean value of seismic energy arriving in the time window considered [25]. The corner frequency f_o was selected as the intersection of the low frequencies level (W_o). A straight line that fits the spectral roll of the slope of the two low frequency bands was used.

3.2.1. Attenuation

Attenuation is the required set of information for estimating spectra in the regional distance. Authors such as Gupta and Nuttli [28] have developed attenuation relations for specific regions and have emphasized the need for developing independent relations for other parts of the world. To determine the attenuation parameter, Q, in the Iranian plateau, Nuttli [29] studied the crustal phases of Iranian earthquakes recorded by stations in Iran. He found a 125 value for P_g, 200 for L_g, and 150 for S_n phases.

The data set for computing the seismic moment comes from broadband records by an *INSN* network, see Figure (5). The portion of the record encompassing the body phase was window tapered with cosine bells in the first and last 10% of the window and then entered into a fast Fourier transform. The *S* wave spectrum was taken from the horizontal component that appeared to have the largest pulse-like signal,

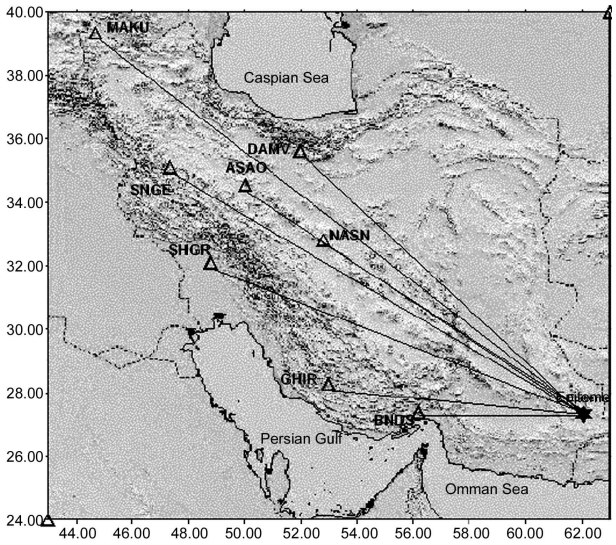

Figure 5. Location of the March 13, 2005 earthquake and INSN Broad Band stations used in this study.

the largest moment, or the component that best fit the Brune model [30]. The spectra were corrected for the effects of filter, instrument response and attenuation parameters, see Figure (6). Average estimates for the multiple stations event were obtained using methods described by Archuleta et al [31]. The source parameters, as well as the letter identification of the event, are given in Table (4).

3.2.2. Source Radius and Stress Drop

Source radius was calculated using a Brune model [30] from the spectral corner frequency (source radius $r_0 = 2.34\ \beta/2\pi f_0$). Final estimates of each source radius were obtained using a linear average of the individual estimates available for that event. Stress drop was obtained by dividing the mean of the

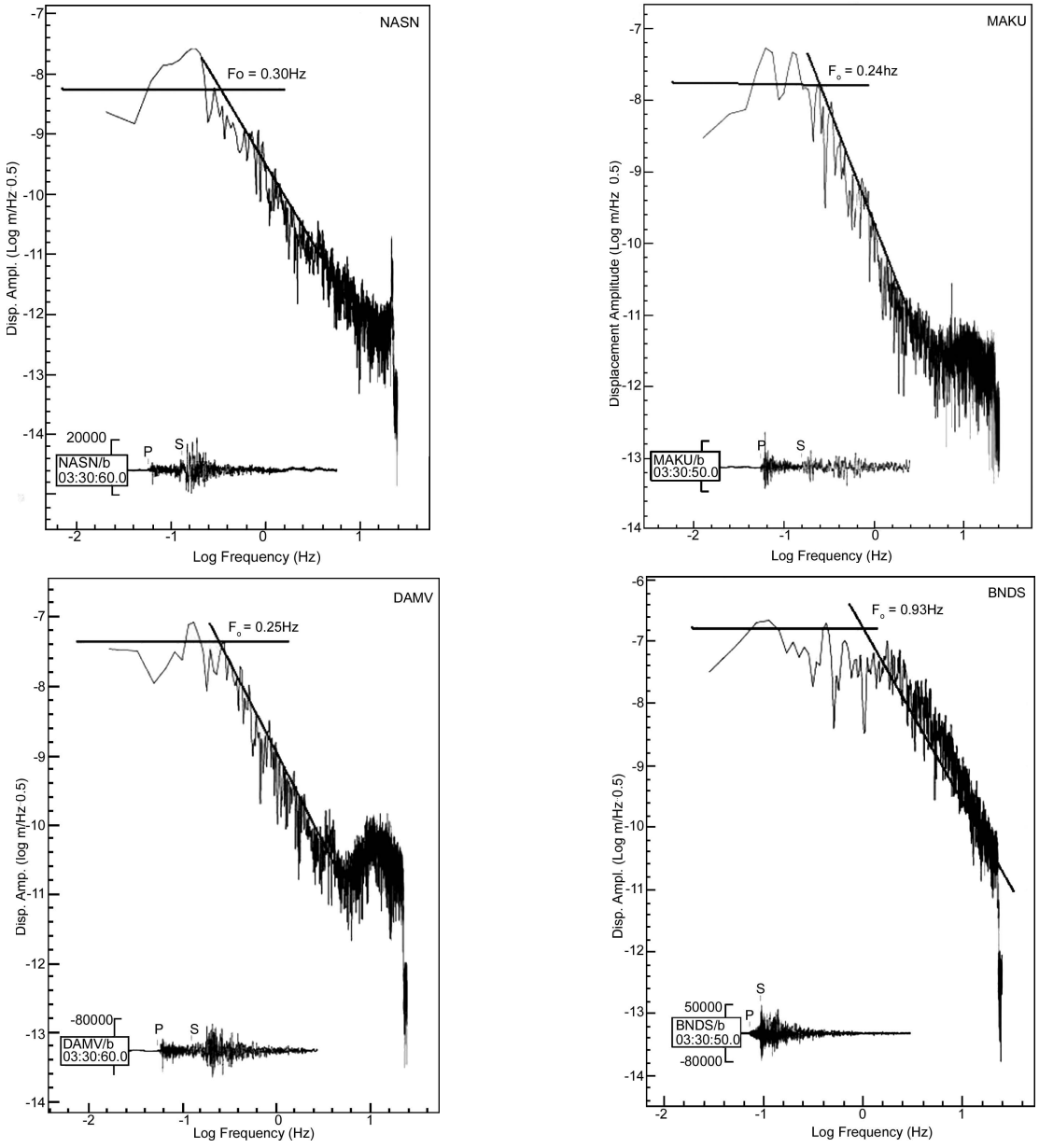

Figure 6. Amplitude spectra prepared using S wave records in INSN stations.

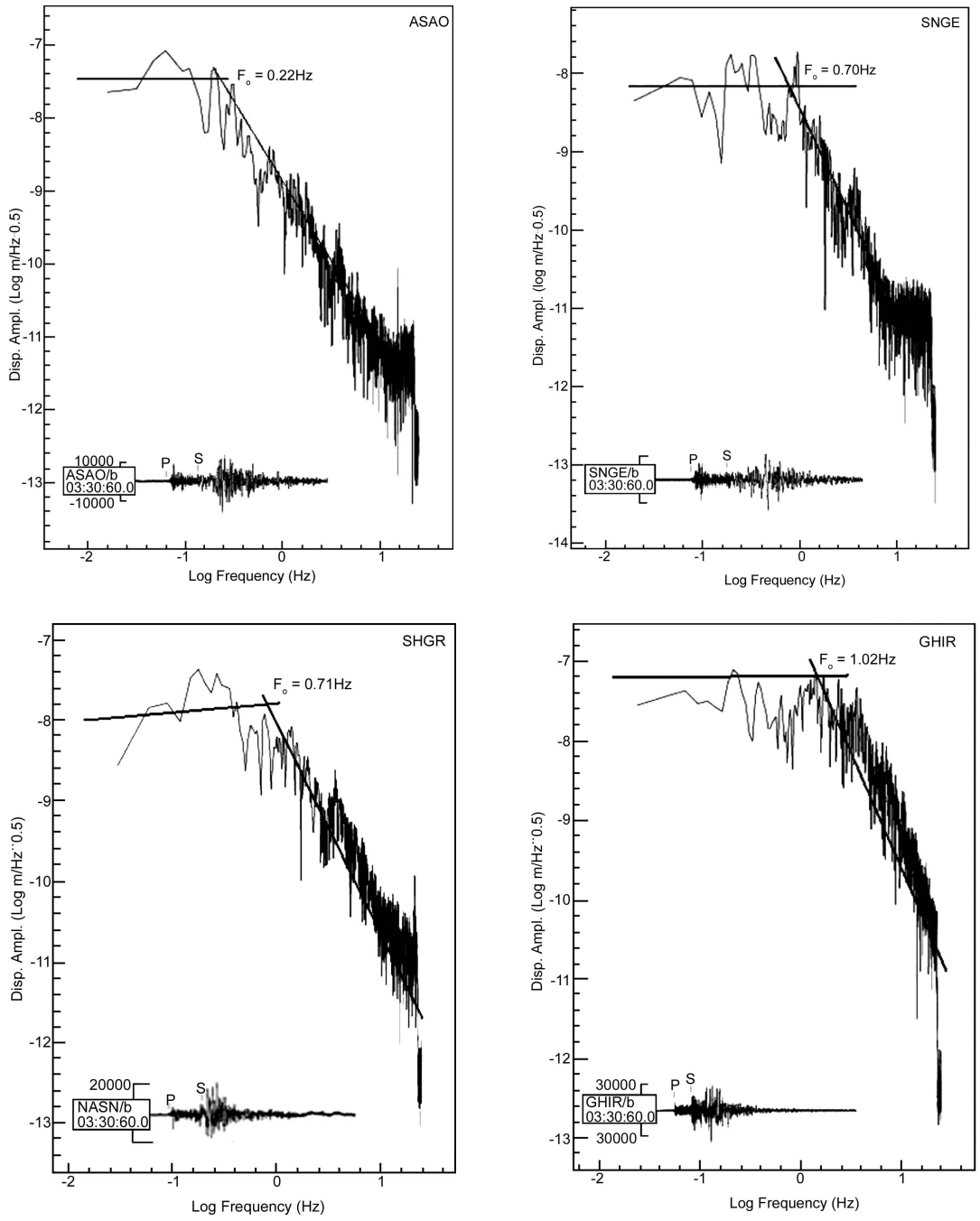

Figure 6. Amplitude spectra prepared using S wave records in INSN stations (Continued...).

Table 4. Source parameters for March 13, 2005 earthquake obtained from spectra.

Station	D ($\times 10^5$cm)	$w_0 \times 10^{-1}$ (cm-sec)	M_O (10^{25}dyne-cm)	f_0 (Hz)
NASN	1390	4.24	7.698	0.30
MAKU	2430	4.40	13.966	0.24
GHIR	1040	5.89	8.001	1.02
DAMV	1760	5.68	13.058	0.25
BNDS	739	7.07	9.235	0.93
ASAO	1700	6.11	13.567	0.22
SNGE	1920	3.41	8.552	0.70
SHGR	1610	4.56	9.589	0.71

moment (M_O) estimates by the cube of the mean of the source radius [32]. Estimates of stress drop ($D\sigma = 7M_O/16r^3$) and source radius are given in Table (5).

Table 5. Source parameters for March 13, 2005 earthquake.

Average Corner Frequency (f_0)	0.54 hz
Source Radius (km)	2.5 km
Average Seismic Moment (dyne-cm)	10.45×10^{25} (This Study) 1.17×10^{25} (CMT)
Stress Drop (bar), (1bar =10^6dyne/cm^2)	0.26×10^4

4. Discussion and Conclusions

From the foregoing, it can be concluded that the earthquake of March 13, 2005 occurred at a source depth of 32*km* and, taking nodal plane two with strike 53^o, were caused by motion on fault plane. Evaluation of previous earthquakes (83 April 18, 1983, January 14, 2003 as reported by Harvard) near to Saravan fault system show that the normal mechanism with strike-slip component and pure normal motion are dominant in this epicenter area. The comparison of focal mechanisms of June 24, 2003 and January 10, 1979 earthquakes (reported by Harvard) with the March 13, 2005 event shows similar normal motion on the fault plane, whereas the strike-slip component occurring on the fault plane during the 1979 event is greater than the March 13, 2005 earthquake. Fault plane solutions of the Makran ranges show that the region is characterized by two seismic regimes [33]: a) shallow earthquakes with thrust mechanism, and b) moderate to deep earthquakes with normal faulting mechanism. No normal fault is observed in the surface but some depression area which is situated in the northern part of the Makran ranges is considered to be downthrown along normal faults [34].

Some discrepancy between Harvard parameters (depth, slip, rake, seismic moment) and source parameters that is calculated in this study can be clearly observed. For shallow earthquakes, the routine Harvard *CMT* solutions, which use the low pass filter data at a 45*s* period, do not accurately resolve the centroid depth. Moreover, since the *CMT* solution is not constrained to be a double-couple source, it often has an intermediate eigenvalue to the moment tensor that is significantly different from the zero value it would have if it was truly double-couple.

Analysis of errors for this model is rather difficult since most errors are undoubtedly associated with unknown deficiencies in the Green functions. Long-duration low-moment far-field pulses are generally associated with low stress drops using Brune model, [30] but this critically is dependent on assumptions of rupture velocities, rise time, and fault area. Errors in the pulse width arise from scattered wave obscuring the true pulse duration and from path effects such as site response. The stress drop of an earthquake must represent the minimum tectonic stress operative to cause the event, as well as a minimum estimate of material strength near the rupture surface.

5. Acknowledgments

I am grateful to Prof. Ghafory-Ashtiany for his support, all reviewers for their useful comments, Dr. Izadkhah for proofreading, and to my colleagues at IIEES for their efforts on the installation and maintenance of the *INSN* seismic network.

References

1. Tirrul, R., Bell, I.R., Griffs, R.I., and Camp, V.E. (1983). "The Sistan Suture Zone of Eastern Iran", *Geol. Soc. Am. Bull.*, **94**, 134-150.

2. Walker, R. and Jackson, J. (2002). "Offset and Evolution of the Gowk Fault, S. E. Iran: A Major Intracontinental Strike-Slip System", *J. Struct. Gel.*, **24**, 1677-1698.

3. Choy, G.L., Boatwright., J., Dewey, J.W., and Sipkin, S.A. (1983). "A Teleseismic Analysis of the New Brunswick Earthquake of January 9, 1982", *J. Geophys. Res.*, **88**, 2199-2212.

4. Choy, G. and Boatwright, J.W. (1988). "Teleseismic and Near Field Analysis of the Nahani Earthquake in the Northwest Territories, Canada", Bull. Seis. Soc. Am., **78**, 1627-1652.

5. Kennet, B.L.N. (1988). Seismological Algorithms, Academic Press, London, 427-440.

6. Jackson, J. and McKenzie, D.P. (1988). "The Relationship Between Plate Motion and Seismic Moment Tensor, and Rates of Active Deformation in the Mediterranean and Middle East", *Geophys. J.*, **93**, 45-73.

7. Taymaz, T., Jackson, J., and McKenzie, D.P. (1991). "Active Tectonics of the North and Central Agean Sea", *Geophys. J. Int.*, **106**, 433-490.

8. Taymaz, T., Eyidogan, H., and Jackson, J. (1991). "Source Parameters of Large Earthquakes in the East Anatolian Fault Zone (Turkey)", *Geophys. J. Int.*, **106**, 537-550.

9. Bullen, K.E. and Bolt, B.A. (1985). "An Introduction to the Theory of Seismology", Cambridge University Press.

10. Aki, K. (1966). D.P. "Generation and Propagation of G Waves from the Niigatu Earthquake of June 16, 1964: Two Estimations of Earthquake

Moment, Released Energy, and Stress Strain Drop From G Wave's Spectrum", Bull. Earthquake Res. Ins., Tokyo University, **44**, 73-78.

11. Berberian, M. (1995). "Natural Hazards and the First Earthquake Catalogue of Iran, 1, Historical Hazards in Iran Prior to 1900". UNESCO/IIEES Publication, UN/IDNDR, IIEES, Tehran, Iran.

12. Berberian, M., Jackson, J.A., Fielding, E., Parsons, B.E., Priestley, K., Qorashi, M., Talebian, M., Walker, R., Wright, T.J., and Baker, C. (2001). "The 1998 March 14 Fandooqa Earthquake (MW6.6) in Kerman Province, Southeast Iran: Re-Rupture of the 1981 Sirch Earthquake Fault Triggering of Slip on Adjacent Thrust and Active Tectonics of the Gowk Fault Zone", *Geophys. J. Int.*, **146**, 371-398.

13. Quttmeyer, R.C. and Jacob, K.H. (1979). "Historical and Modern Seismicity of Pakistan, Afghanistan, Northwestern India, and Southeastern Iran", Bull. Seis. Soc. Am., **69**(3), 773-823.

14. Berberian, M., Jackson, J.A., Qorashi, M., Talebian, M., Khatib, M., and Priestley, K. (2000). "The 1994 Sefidabeh Earthquakes in Eastern Iran: Blind Thrusting and Bedding-Plane Slip on a Growing Anticline and Active Tectonics of the Sistan Suture Zone", *Geophys. J. Int.*, **142**, 283-299.

15. Jackson, J.A., Harris, A.J., and Holt, W.E. (1995). "The Accommodation of Arabia-Eurasia Plate Convergence in Iran", *J. Geophys. Res.*, **106**, 15205-15219.

16. McCaffery, R., Abers, G., and Zwick, P. (1991). "Inversion of Teleseismic Body Waves", Digital Seismogram Analysis and Waveform Inversion, W.H.K. Lee, ed., PEI Software Library, **3**, 81-166.

17. Nabelek, J.L. (1984). "Determination of Earthquake Source Parameters from Inversion of Body Waves", Ph.D. Thesis, MIT, Cambridge, Massachusetts.

18. Futterman, W.I. (1962). "Dispersive Body Waves", *J. Geophys. Res.*, **67**, 5279-5291.

19. Carpenter, E.W. (1966). "Absorption of Elastic Waves as an Operator for a Constant Mechanism", Atomic Weapons Research Establishment Report 0-4366, Her Majesty's Station Office, London.

20. Molnar, P. and Lyon-Caen, H. (1989). "Fault Plane Solutions of Earthquakes and Active Tectonics of the Tibetan Plateau and its Margin", *Geophys. J. Int.*, **99**, 123-153.

21. Maggi, A., Jackson, J.A., Priestley, K., and Baker, C. (2000). "A Reassessment of Focal Depth Distributions in Southern Iran, the Tien Shan and Northern India: Do Earthquakes Really Occur in the Continental Mantle?", *Geophys. J. Int.*, **143**, 629-661.

22. Walker, R., Jackson, J., and Baker, C. (2004). "Active Faulting and Seismicity of the Dasht-e-Bayaz Region, Eastern Iran", *Geophys. J. Int.*, **157**, 265-282.

23. Aki, K. (1969). "Analysis of the Seismic Coda of Local Earthquake as Scattered Waves", *J. Geophys. Res.*, **74**, 615-631.

24. Aki, K. and Chouet, B. (1975). "Origin of Coda Waves: Source, Attenuation and Scattering Effects", *J. Geophys. Res.*, **80**, 3322-3342.

25. Bolt, B.A. and Herraiz, M. (1983). "Simplified Estimation of Seismic Moment from Seismograms", *Bull. Seis. Soc. Am.*, **73**(3), 735-748.

26. Keilis-Borok, V.I. (1960). "Investigation of the Mechanism of Earthquakes" (English Translation), *Soc. Res. Geophys.*, **4**, 29.

27. Riznichenko, Y.V. (1992). "Problems of Seismology", Mir Publisher Moscow, 3-27.

28. Gupta, I.N. and Nuttli, O.W. (1976). "Spatial Attenuation of Intensities for Central US Earthquakes", Bull. Seis. Soc. Am., **66**, 473-751.

29. Nuttli, O.W. (1980). "The Excitation and Attenuation of Seismic Crustal Phases in Iran", Bull. Seis. Soc. Am., **70**(2), 469-485.

30. Brune, J.N. (1970). "Tectonic Stress and Spectra of Seismic Shear Waves from Earthquakes", *J. Geophys. Res.*, **75**, 4997-5009.

31. Archuleta, R., Cranswick, E., Muller, C., and Spudich, P. (1982). "Source Parameters of the 1980 Mammoth Lake, California Earthquake Sequence", *J. Geophys. Res.*, **87**, 4595-4607.

32. Fletcher, J.B. (1980). "Spectra for High Dynamic Range Digital Recordings of Oroville, California Aftershocks and their Source Parameters", Bull. Seis. Soc. Am., **70**(3), 735-755.

33. Jacob, K.H. and Quittmeyer, R.C. (1979). "The Makran of Pakistan and Iran: Trench-arc System with Active Plate Subduction", Geodynamics of Pakistan, Farah, A. and De Jong, K. (eds.), *Geol. Survey of Pakistan*, 305-317.

34. Farhudi, G. and Karig, D.E. (1977). "Makran of Iran and Pakistan as an Active Arc System", *Geol.*, **5**(11), 664-668.